and maintenance of genomic stability. P53 mutation is shown to be associated with the progression of HCC from an early to a more advanced stage.[1] In HCC developed from populations exposed to AFB1, specific TP53 mutation R249S is observed in more than 50% of the tumours.[1] Microsatellite instability (MSI) occurs in hepatocytes in some cases of chronic hepatitis, cirrhosis, and HCC.[8,9] Alterations in DNA mismatch repair genes involved in MSI have also been found in HCC, especially HCV-associated HCC.[10] In this way, genetic alterations involved in some of the multi-steps in carcinogenesis have been elucidated to some extent in recent years. Understanding of the molecular mechanisms of HCC development is very important for the improvement in prevention, treatment strategies and prognosis of HCC.

There have been great recent advances made in treatment of HCC, but the long-term prognosis after curative resection of HCC remains poor. One of the primary reasons for poor prognosis following curative resection is the high recurrence rate—roughly 20–30% within 1 year and 80% in 5 years.[11,12] Intrahepatic recurrences arise from either intrahepatic metastases or multicentric occurrences. Recurrences due to intrahepatic metastases are generally found to be more aggressive than those from multicentric occurrences possibly because intrahepatic metastases are in a later stage of hepatocarcinogenesis than those of multicentric occurrences, which can be considered *de novo* tumours.[13,14] Distinction of these two types of recurrence is important not only for understanding the biological process of liver carcinogenesis, but also for determining the optimal treatment for the patient.

Our previous study showed that most mutations of not only *p53* but also *hMSH2* genes occurred in moderately or poorly differentiated HCCs, suggesting that the presence of either a *p53* or *hMSH2* gene mutation is involved in the tumour progression of HCC.[4] It was also suggested that lack of mutations in both *p53* and *hMSH2* closely correlates with the survival in HCC patients treated by surgery.[4] Among DNA mismatch repair genes, there seems close interaction between p53 and hMSH2 proteins during carcinogenesis. First, p53 alterations are associated with altered expression of MMR protein, namely hMSH2 protein.[7,15] Second, MSI inversely correlates with the presence of *p53* mutation in tumours.[16] Third, the presence of p53 response element in the *hMSH2* proximal promoter suggests that p53 regulates hMSH2 expression.[17,18] Fourth, p53 overexpression was associated with upregulation of hMSH2 protein.[7,15] Therefore, we hypothesise that alterations of p53 and hMSH2 genes may be associated with not only survival in HCC patients but also recurrence of HCC following curative resection.

The purpose of this study is to examine the effects of deficiencies of *p53* and *hMSH2* gene function on the development of recurrences of HCC and overall survival following curative resection and establish a relatively simple predictive assay which may be of value in the clinical care of HCC patients.

2. Materials and methods

2.1. *Subjects*

We obtained tissue samples by surgical resection from 83 HCC patients, in all cases with their informed consent. Histopathologic examination of haematoxylin-eosin stained, paraffin-embedded sections was performed for all patients. Tumours were histologically classified into well, moderately, and poorly differentiated HCC according to the criteria of Edmondson and Steiner.[19] Histological grading is classified by acidophilic cytoplasm, nuclear/cytoplasm ratio and arrangement of neoplastic cell. No patient was lost to follow-up. The duration of follow-up period is 36–105 months. The patient group consisted of 67 men and 16 women (ages 48–77 years; mean 63.0 ± 7.0). Serological testing for serum hepatitis B virus surface antigen was positive in 13 patients (15.7%), and serum anti-hepatitis C virus antibody was present in 64 patients (77.1%); we also found that two patients (2.4%) were positive for both markers and four patients (4.8%) were negative for both. Fifty of our patients (60.2%) had cirrhosis. Times to relapse and survival were measured from the date of surgery. For survival analyses, one patient who died of disease complication within a month of surgery and three patients whose resections were non-curative were excluded.

2.2. *DNA isolation*

Samples of dissected tumours and surrounding non-cancerous tissues were frozen in liquid nitrogen and stored at −80 °C until their DNA was extracted. Genomic DNA was digested with SDS and proteinase K prior to extraction with phenol–chloroform and precipitation with ethanol. After extraction, the purified DNA was stored at 4 °C.

2.3. *Single-strand conformational polymorphism (SSCP)*

To screen the *hMSH2* and *p53* genes for variant sequences, we performed SSCP analysis by the method of Orita and colleagues[20], with particular emphasis on all coding exons of the *hMSH2* gene as well as exons 5–8 of the *p53* gene. The PC primers for amplification of each exon of *hMSH2* and *p53*, and the polymerase chain reaction (PCR) conditions were as previously described.[21,22] PCR-amplified fragments were heat denatured at 95 °C for 10 min and then loaded on to 8% non-denaturing polyacrylamide gels maintained at 5 °C; the gels were dried and exposed to X-ray film. Samples exhibiting altered SSCP migration patterns were subjected to direct nucleotide sequencing.

2.4. *Direct nucleotide sequencing*

After purification of the PCR products, the products were used as templates for sequencing. For *p53*, the PCR products were denatured to produce single-stranded templates before fluorescence sequencing was performed in an automated sequencing system (ALFred DNA Sequencer, Pharmacia LKB, Uppsala, Sweden). The dideoxy chain-termination method and the Thermo sequenase fluorescent labelled primer cycle sequencing kit were used (Amersham Life Science, Little Chalfont, England).

2.5. *Statistics*

The Chi-square or Fisher's exact test was used to evaluate the statistical significance of categorical variables. Cumulative

disease-free and survival rates were estimated by the method of Kaplan and Meier. The statistical significance of differences in the survival curves of different subgroups was analysed by the log-rank test. The overall survival of the study variables was assessed using the Cox proportional hazards model. Multiple group comparisons were conducted by one-way analysis of variance (ANOVA), followed by Tukey's honestly significant difference (HSD) test. These statistic analyses were performed with SPSS ver. 11.5J software.

3. Results

3.1. *Mutations of the p53 and hMSH2 genes in HCC*

We screened the genomic DNA from 83 HCC patients for somatic mutations in the *p53* and *hMSH2* genes by both PCR–SSCP and direct sequencing using primer sets shown in Table 1. Tables 2 and 3 summarise results of these mutations. We detected mutations of the *p53* gene in 16/83 patients (19.3%); 12 of the 16 mutations were missense, three were deletions and one was nonsense (Table 2). Among these *p53* mutations, we found triple missense mutations in one case (#57) and double ones in another (#69) (Table 2). On the other hand, point mutations of the *hMSH2* gene were found in 9/83 patients (10.8%) (Table 3). Only one patient had both *p53* and *hMSH2* gene mutations in his tumour.

3.2. *Clinico-pathological characteristics by mutation status of p53 and hMSH2 genes*

To assess the association of mutation status of *p53* and *hMSH2* genes with clinico-pathological characteristics, HCC patients were divided into three groups; namely, those with *p53* mutation ($n = 16$) including one case possessing both *p53* and *hMSH2* mutations, with *p53* wild/*hMSH2* mutation ($n = 8$), and with *p53* wild/*hMSH2* wild ($n = 59$). Presence or absence of intrahepatic metastasis (im) showed a significant heterogeneity in the distribution of number of patients among three groups ($P = 0.026$, chi-square test) (Table 4). In addition, when compared HCC patients harbouring *p53* and/or *hMSH2* mutations and those without mutations, there was a significant difference only for im ($P = 0.015$, Fisher's exact test) (Table 4).

Table 2 – Mutations of *p53* gtene in HCC

Case No.	Exon	Codon	Nucleotide alterations	Amino acid substitutions
4	6	220	TAT → TGT	Tyr → Cys
6	7	237	ATG → ATT	Met → Ile
25	5	176	TGC → TAC	Cys → Tyr
31	5	164	AAG → TAG	Lys → Stop
32	7	246	ATG → GTG	Met → Val
35	8	281	GAC → TAC	Asp → Tyr
39	6	189	1 bp deletion (frame shift)	
42	5	146	TGG → TGT	Trp → Cys
44	8	283	1 bp deletion (frame shift)	
52	5	155	ACC → ATC	Thr → Ile
56	6	214	CAT → CGT	His → Arg
57	6	200	AAT → AGT	Asn → Ser
	6	205	TAT → TCT	Tyr → Ser
	6	207	GAT → GCT	Asp → Ala
68	7	238	TGT → CGT	Cys → Arg
69	5	173	GTG → ATG	Val → Met
	5	175	CGC → ATG	Arg → Cys
72	5	154–157	9 bp deletion	
76	5	155	ACC → ATC	Thr → Ile

Table 1 – Oligonucleotide primer sequences used for detection of alterations of *p53* and *hMSH2* genes

p53	Sense (5′ → 3′)	Antisense (5′ → 3′)	Length (bp)
Exon 5	TCCTACAGTACTCCCCTGCC	GCCCCAGCTGCTCACCATC	207
Exon 6	ACTGATTGCTCTTAGGTCTG	AGTTGCAAACCAGACCTCAG	143
Exon 7	AGGTTGGCTCTGACTGTACC	GTCGTGACCTGGAGTCTTGC	120
Exon 8	CTATCCTGAGTAGTGGTAATC	GTCCTGCTTGCTTACCTCGC	165
hMSH2	Sense (5′ → 3′)	Antisense (5′ → 3′) Length	(bp)
Exon 1	TCGCGCATTTTCTTCAACCA	TCCCTCCCCAGGACG	284
Exon 2	TTTTTTGAGCAAAGAATCTGC	ACCTTATATGCCAAATACCAATC	162
Exon 3	TTAGGCTTCTCCTGGCAATC	CCTTTCCTAGGCCTGGAATC	332
Exon 4	CTTATTCCTTTTCTCATAGTAGT	TTGTAATTCACATTTATAATCCATG	221
Exon 5	GCTATAGGAAATCTTCGATTTTTA	TACCTAAAAAGGTTAAGGGCTC	193
Exon 6	TGAGCTTGCCATTCTTTCTATT	TGGGTAACTGCAGTTACATAAA	225
Exon 7	TTCAGATTGAATTTAGTGGAAGC	AGCTTCATGTTTTTCCAGAGC	207
Exon 8	TTTGTTTTACTACTTTCTTTTAGG	AAGTATATTGCATACCTGATCC	148
Exon 9	TAATTTCTGTCTTTACCCATTATTT	CAACCTCCAATGACCCATTC	204
Exon 10	TGGTAGTAGGTATTTATGGAATAC	ATCATGTTTAAGAGCATTTAGGG	264
Exon 11	TACACATTGCTTCTAGTACAC	AGCCAGGTGACATTCAGAAC	202
Exon 12	ATTATTCAGTATTCCTGTGTAC	ACCCCCACAAAAGCCCAAA	326
Exon 13	ATTTATTAGTAGCAGAAAGAAGTT	AAGGGACTAGGAGATGCAC	287
Exon 14	GTTACCACATTTTATGTGATGG	TTCTGAATTTAGAGTACTCC	329
Exon 15	TCTCATGCTGTCCCCTCAC	AAGTTAAACTATGAAAACAAACTG	247
Exon 16	ACTAATGGGACATTCACATGTG	TCAATATTACCTTCATTCGATTAC	232

Table 3 – Mutations of MSH2 gene in HCC

Case No.	Exon	Codon	Nucleotide alterations	Amino acid substitutions
1	1	45	GCG → GTG	Ala → Val
14	7	390	CTT → TTT	Leu → Phe
22	7	390	CTT → TTT	Leu → Phe
	12	629	CAA → CGA	Gln → Arg
33	14	803	ACA → GCA	Thr → Ala
39	3	180	CCA → ACA	Pro → Thr
59	3	180	CCA → TCA	Pro → Ser
64	3	191	CAT → CGT	His → Arg
73	3	180	CCA → ACA	Pro → Thr
81	3	180	CCA → ACA	Pro → Thr

Except for the im, none of the other variables showed any difference among these groups.

3.3. *Disease-free survival*

We conducted univariate analysis for disease-free survival (DFS) in all 79 HCC patients with follow-up data available (Table 5). Presence or absence of *p53* mutation showed a significant difference of DFS period (median: 5 versus 48 months, $P < 0.0001$, log-rank test). On the other hand, other variables including *hMSH2* mutation did not show any significant differences for DFS. Since *p53* mutation status was such a strong prognostic factor, stratification of HCC patients by *p53* mutation status is required not to overlook other prognostic factors. We then analysed only for 65 HCC patients without *p53* mutation. Notably, HCC patients with *hMSH2* mutation showed a significantly shorter DFS than those without the mutation (18 versus 58 months, $P = 0.019$). In addition, liver cirrhosis showed a marginal significance among 65 HCC patients with wild *p53* ($P = 0.075$, log-rank test).

Comparisons of DFS among three groups of HCC patients with *p53* mutation ($n = 14$), those with *p53* wild/*hMSH2* mutation ($n = 8$) and those without mutation ($n = 57$) are shown using Kaplan–Meier survival curves (Fig. 1). The 3-year DFS rates of HCC patients were 14.3%, 37.5% and 67.5%, respectively.

In the multivariate analysis, categories by *p53* and *hMSH2* mutation status and liver cirrhosis that showed $P < 0.1$ in univariate analysis were included as explanatory variables (Table 6). HCC patients with *p53* wild/*hMSH2* mutation and those with *p53* mutation showed 2.9- and 7.3-fold risks as compared with those without mutation ($P = 0.014$, $P < 0.001$, respectively). In addition, liver cirrhosis also showed a statistically significant difference ($P = 0.025$) in the analysis.

3.4. *Association of recurrent patterns and mutation status of p53 and hMSH2 genes*

Recurrence was detectable in 45 of 79 patients (57.0%). As shown in Table 7, frequency of recurrence in *p53* and/or *hMSH2* mutation group was significantly higher than that in the *p53* wild/*hMSH2* wild group (87.0% versus 44.6%, $P = 0.001$). Moreover, interestingly, the frequency of patients

Table 4 – Clinico-pathological and epidemiological features stratified by *p53* and *hMSH2* mutation status

		p53 wild/*hMSH2* wild (Reference) ($n = 59$)	*p53* mutation ($n = 16$)	*p53* wild/*hMSH2* mutation $n = 8$	p^{*}	*p53* and/or *hMSH2* mutation ($n = 24$)	p^{**}
Gender	Female (*n*)	11	3	2	0.9	5	1
	Male (*n*)	48	13	6		19	
Age	⩽69 yrs (*n*)	45	15	5	0.2	20	0.6
	⩾70 yrs (*n*)	14	1	3		4	
Tumour size	<2 cm (*n*)	10	0	1	0.2	1	0.2
	>2 cm (*n*)	49	16	7		23	
Differentiation	Well (*n*)	11	0	1	0.2	1	0.2
	Moderately/Poorly (*n*)	48	16	7		23	
HBs Ab	Negative (*n*)	48	14	7	0.8	21	0.7
	Positive (*n*)	11	2	1		3	
HCV	Negative (*n*)	15	3	1	0.6	4	0.6
	Positive (*n*)	44	13	7		20	
Liver cirrhosis	Negative (*n*)	20	9	4	0.2	13	0.1
	Positive (*n*)	39	7	4		11	
Intrahepatic metastasis	Negative (*n*)	36	4	3	0.026	7	0.015
	Positive (*n*)	23	12	5		17	
Portal vein involvement (*n*)	Negative (*n*)	39	7	5	0.3	12	0.2
	Positive (*n*)	20	9	3		12	

im, intrahepatic metastasis; vp, portal vein invasion.
* Chi-square test for 2 × 3 table.
** Fischer's exact test for 2 × 2 table (*p53* wild/*hMSH2* wild versus *p53* and/or *hMSH2* mutation).

Table 5 – Prognostic factors of disease-free and overall survival by uni variate analysis

Variables		All (n = 79)					Only p53 wild (n = 65)				
		No. of Patients	DFS		OS		No. of Patients	DFS		OS	
			Median (months)	P*	Median (months)	P*		Median (months)	P*	Median (months)	P*
Gender	Female (n)	16	36	0.9	67	0.5	13	41	0.9	98	0.9
	Male (n)	63	44		–		52	48		–	
Age	⩽69 yrs (n)	61	40	0.4	78	0.8	48	47	0.8		0.9
	⩾70 yrs (n)	18	48		98		17	48		98	
Tumour size	<2cm (n)	10	44	0.2	–	0.3	10	44	0.5	–	0.6
	⩾2cm (n)	69	38		78		55	48		98	
Differentiation	Well (n)	12	44	0.5	67	0.7	12	44	0.9	67	0.7
	Moderately/Poorly (n)	67	41		98		53	58		98	
HBs Ag	Negative (n)	65	40	0.9	78	0.3	53	48	0.9	98	0.4
	Positive (n)	14	44		–		12	47		–	
HCV	Negative (n)	18	58	0.2	–	0.068	16	58	0.2	–	0.1
	Positive (n)	61	32		67		49	44		98	
Liver cirrhosis	Negative (n)	33	47	0.3	–	0.037	24	–	0.075	–	0.008
	Positive (n)	46	32		61		41	41		67	
im	Negative (n)	42	44	0.5	98	0.7	38	47	1.0	98	1.0
	Positive (n)	37	36		78		27	48		–	
vp	Negative (n)	49	44	0.7	–	0.1	43	47	0.6	–	0.4
	Positive (n)	30	20		78		22	–		98	
p53	Wild (n)	65	48	<0.0001	98	<0.0001					
	Mutated (n)	14	5		24						
hMSH2	Wild (n)	70	44	0.3	98	0.3	57	58	0.019	98	0.011
	Mutated (n)	9	21		–		8	18		30	

DFS, disease-free survival; OS, overall survival; im, intrahepatic metastasis; vp, portal vein invasion.
A dash (-) indicates that the median survival could not be calculated because the last cumulative survival was greater than 50%.
* Log-rank test.

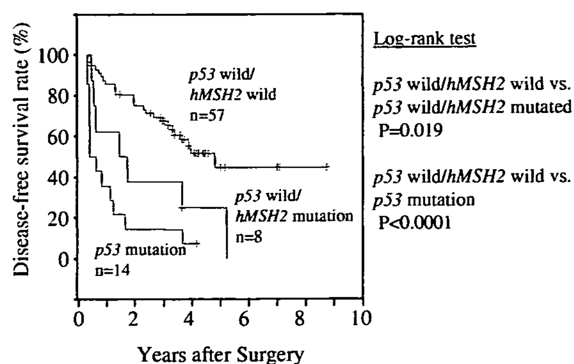

Fig. 1 – The Kaplan–Meier curves for disease-free survival for the three groups of HCC patients after a curative resection are shown: patients with *p53* mutation, those with *p53* wild/*hMSH2* mutation and those with *p53* wild/*hMSH2* wild.

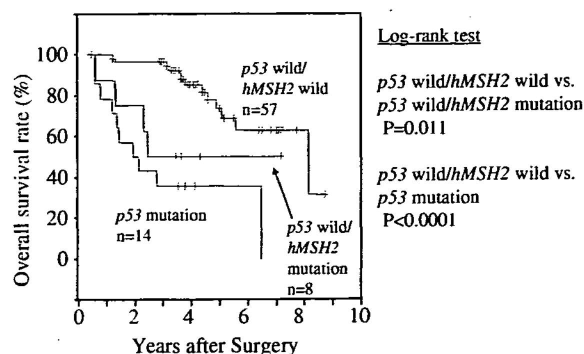

Fig. 2 – The Kaplan–Meier curves for overall survival for the three groups of HCC patients after a curative resection are shown: patients with *p53* mutation, those with *p53* wild/*hMSH2* mutation and those with *p53* wild/*hMSH2* wild.

Table 6 – The multivariate analysis of disease-free survival by means of the Cox's proportional hazard model

Variables		Risk ratio (95% CI)	P
Gene mutations	p53 wild/MSH2 wild	1 (reference)	
	p53 wild/MSH2 mutation	2.929 (1.241–6.915)	0.014
	p53 mutation	7.328 (3.470–15.474)	< 0.001
Liver cirrhosis	Negative	1 (reference)	
	Positive	2.106 (1.097–4.044)	0.025

with p53 and/or hMSH2 mutations in intrahepatic metastasis (75.0%) was significantly higher than that in multicentric occurrence (14.3%) (P = 0.001, respectively, Tukey's HSD test).

3.5. *Overall survival*

We also conducted univariate analysis for overall survival (OS) in all 79 HCC patients (Table 5). HCC patients with p53 mutation demonstrated a significantly shorter OS than those without (24 versus 98 months, P < 0.0001). In addition, liver cirrhosis also showed a significant difference (P = 0.037), while a marginal significance of OS was found for HCV status (P = 0.068).

We next analysed OS using only 65 HCC patients without p53 mutation as described above. Remarkably, HCC patients with hMSH2 mutation showed a significantly shorter OS compared with those without the mutation (30 versus 98 months, P = 0.011). Comparisons of OS among HCC patients with *p53* mutation (*n* = 14), those with p53 wild/*hMSH2* mutation (*n* = 8) and those without mutation (*n* = 57) are also shown in Fig. 2. The 3-year OS rates of HCC patients were 35.7%, 50.0% and 96.4%, respectively.

In the multivariate analysis, we included categories by p53 and *hMSH2* mutation status, HCV and liver cirrhosis as explanatory variables that showed P < 0.1 in univariate analysis (Table 8). HCC patients with *p53* wild/*hMSH2* mutation and those with *p53* mutation showed 6.8- and 14.5-fold risks compared with those without mutation (P = 0.003, P < 0.001, respectively). In addition, liver cirrhosis also revealed a statistically significant difference (P < 0.001). On the other hand, HCV did not show significance for OS in the analysis.

Table 7 – Recurrent pattern in HCC patients by status of p53 or hMSH2 mutation

		p53 and/or hMSH2 mutations	p53 wild/ hMSH2 wild	Frequency of mutated patients (%)	P
Recurrence	Intrahepatic recurrence				0.001*
	Intrahepatic metastasis (n)	12	4	75.0	0.001**
	Multicentric occurrence (n)	2	12	14.3	
	Unclassified (n)	1	4	20.0	
	Distant metastasis (n)	5	5	50.0	
	Total (n)	20	25	44.4	<0.001***
No recurrence		2	32	5.9	

* One way ANOVA for patients with intrahepatic recurrence.
** Tukey's HSD test for intrahepatic metastasis versus multicentric occurrence.
*** Fisher's exact test for recurrence versus no recurrence.

Table 8 – The multivariate analysis of overall survival by means of the Cox's proportional hazard model

Variable		Risk ratio (95% CI)	p
Gene mutations	p53 wild/MSH2 wild	1 (reference)	
	p53 wild/MSH2 mutation	6.813 (1.894–24.505)	0.003
	p53 mutation	14.504 (5.240–40.147)	0.001
Liver cirrhosis	Negative	1 (reference)	
	Positive	6.544 (2.298–18.637)	0.001
HCV	Negative	1 (reference)	
	Positive	3.060 (0.764–12.255)	0.11

4. Discussion

This study presents the results of an analysis of the clinical features of hepatocellular carcinoma in 83 HCC patients with and without *p53* and/or *hMSH2* mutations. Interestingly, HCC patients without mutations of these genes showed a better prognosis including recurrence and survival than those with gene mutations. Furthermore, *p53* or *hMSH2* mutation status was also found to be associated with the pattern of recurrence. These findings suggest that mutations of these genes may be deeply involved in not only the progression of HCC but also the recurrence development of HCC.

A *p53* or *hMSH2* gene mutation may accelerate the progressional development of HCC by a 100–600-fold increase in the rate of spontaneous mutations and accumulation due to defects in mismatch repair.[23,24] It is of course also possible that the loss of a mismatch repair function is likely to lead to high frequencies of ectopic recombination[25,26]; this may then lead to genomic rearrangement(s) and, as a result, activation of an oncogene or inactivation of a tumour suppressor gene, resulting in the acceleration of progression of HCC.

On the other hand, although *p53* or *hMSH2* mutation were not detected in non-malignant cells in cancer tissue, prognosis of the patients was worse than that without the mutations. This may be because the genome in normal cells around tumours is more instable in HCCs with *p53* or *hMSH2* mutation than those without these mutations, influencing the recurrence or survival. The possibility cannot be excluded that a few normal cells with *p53* or *hMSH2* mutation have existed within cancer tissue though we cannot detect these mutations by our assay system.

Cells in a tumour may well become resistant to chemotherapeutic agents following their acquisition of mutations that affect the *p53* or *hMSH2* genes[27–29]; this is because it should be much easier for cells that have a disrupted mismatch repair system to acquire a drug resistance phenotype by virtue of the increased mutability which stems from their genomic instability. Thus there may be significant differences in responsiveness to chemotherapy in HCC patients with *p53* and/or *hMSH2* mutations and without these mutations, and this could well lead to their experiencing significantly different survival periods following a relapse.

The recurrent tumours identified in this study were classified in accordance with the recommendations of the Liver Cancer Study Group of Japan in their paper on the classification of primary liver cancers.[30] Thus the term intrahepatic metastasis is used to describe: 1) tumours that can be clearly seen as having grown from portal vein tumour thrombi, 2) tumours that surround a large main tumour with multiple satellite nodules, and 3) a small solitary tumour which is close to the main tumour and is either histologically similar to or less differentiated than the main tumour. Multiple HCC lesions that cannot be described as metastases under the above criteria are believed to represent potential multicentric occurrences; such tumours are separately recorded as *'de novo carcinogenesis'*. However, there may often be recurrent tumours that are difficult to classify as either intrahepatic metastases or multicentric

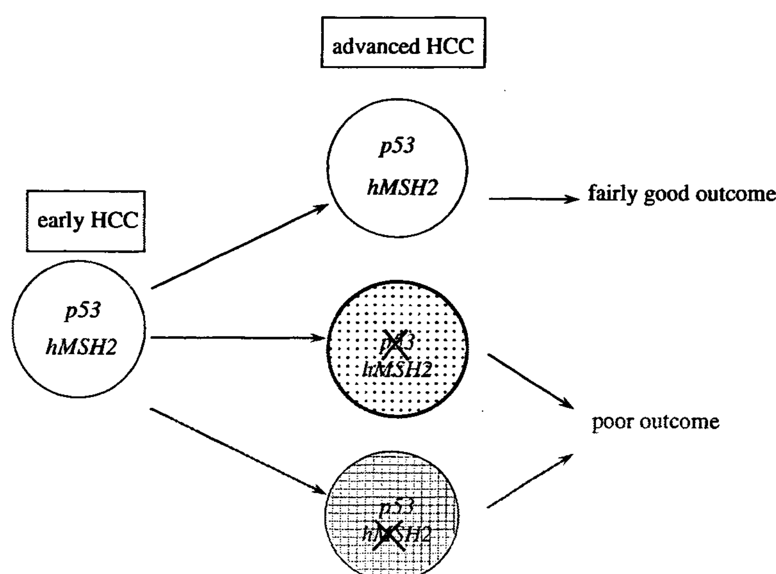

Fig. 3 – A proposed model of hepatocellular carcinogenesis with emphasis on progression in relation to mutations of *p53* and *hMSH2* genes.

occurrences. Several studies have tried to examine the possible histologic[14] and genetic[31–33] differential diagnoses, but this is still impossible. In our present study, almost all of the cases in which we found a *p53* and/or an *hMSH2* gene mutation appeared to relapse within 2 years of surgery as a consequence of intrahepatic metastasis. Although we noted that the outcomes were reasonably good in the great majority of the *p53* wild/*hMSH2* wild cases, there were a few cases involving multicentric occurrence that led to relapses occurring 3-plus years after surgery. Frequency of multicentric occurrence was also higher in *p53* wild/*hMSH2* wild cases than in these mutation positive cases. These findings suggest that gene alterations other than mutations of *p53* and *hMSH2* may be involved in recurrence and survival. So, gene alterations, especially on DNA repair system including other mismatch repair genes, need to be analysed.

Fig. 3 summarises the situation as we found it in patients with HCC. There seemed to be relatively few mutations in either *p53* or *hMSH2* in early-stage HCCs. The early-stage HCCs then developed into advanced-stage HCCs, which were more than 2 cm in diameter and were either poorly or moderately de-differentiated. The outcome tended to be pretty poor in those HCC patients whose tumours showed clear evidence of *p53* or *hMSH2* mutations, whereas in patients whose tumours had no mutation of either gene the outcome tended to be somewhat better.

Conflict of interest statement

None declared.

Acknowledgement

The authors thank Dr. K. S. Iwamoto, UCLA, for discussions. We are also grateful to: Shiho Yano and Chiyoe Saitoh for excellent technical help.

This is part of a collaborative study between the liver disease projects of the Department of Surgery, Division of Frontier Medical Science, Graduate School of Biomedical Sciences, Hiroshima University and the Radiation Effects Research Foundation (RERF), Hiroshima, Japan. RERF is a private, nonprofit foundation funded equally by the Japanese Ministry of Health and Welfare and the U.S. Department of Energy through the National Academy of Sciences.

REFERENCES

1. Suriawinata A, Xu R. An update on the molecular genetics of hepatocellular carcinoma. *Semin Liver Dis* 2004;**24**:77–88.
2. Sun M, Eshleman JR, Ferrell LD, et al. An early lelsion in hepatic carcinogenesis: Loss of heterozygosity in human cirrhotic livers and dysplastic nodules at the 1p36-p34 region. *Hepatology* 2001;**33**:1415–24.
3. Yeh SH, Chen PJ, Shau WY, et al. Chromosomal allelic imbalance evolving from liver cirrhosis to hepatocellular carcinoma. *Gastroenterology* 2001;**121**:699–709.
4. Yano M, Asahara T, Dohi K, Mizuno T, Iwamoto KS, Seyama T. Close correlation between a p53 or hMSH2 gene mutation in the tumor and survival of hepatocellular carcinoma patients. *Int J Oncol* 1999;**14**:447–51.
5. Katiya S, Dash BC, Thakur V, Guptan RC, Sarin SK, Das BC. P53 tumor suppressor gene mutations in hepatocellular carcinoma patients in India. *Cancer* 2000;**88**:1565–73.
6. Wang L, Bani-Hani A, Montoya D, et al. hMLH1 and hMSH2 expression in human hepatocellular carcinoma. *Int J Oncol* 2001;**19**:567–70.
7. Hussein MR. Alterations of p53, Bcl-2, and hMSH2 protein expression in the cirrhotic, macroregenerative, dysplastic nodules and hepatocellular carcinomas in upper Egypt. *Liver Int* 2004;**24**:552–60.
8. Salvucci M, Lemoine A, Saffroy R, et al. Microsatellite instability in European hepatocellular carcinoma. *Oncogene* 1999;**18**:181–7.
9. Macdonald GA, Greenson JK, Saito K, Cherian SP, Appelman HD, Boland CR. Microsatellite instability and loss of heterozygosity at DNA mismatch repair gene loci occurs during hepatic carcinogenesis. *Hepatology* 1998;**28**:90–7.
10. Zekri AR, Sabry GM, Bahnassy AA, Shalaby KA, Abdel-Wahabh S, Zakaria S. Mismatch repair genes (hMLH1, hPMS1, hPMS2, GTBP/hMSH6, hMSH2) in the pathogenesis of hepatocellular carcinoma. *World J Gastroenterol* 2005;**11**:3020–6.
11. Shimada M, Takenaka K, Gion T, et al. Prognosis of recurrent hepatocellular carcinoma: A 10-year surgical experience in Japan. *Gastroenterology* 1996;**111**:720–6.
12. Sugimachi K, Maehara S, Tanaka S, Shimada M, Sugimachi K. Repeat hepatectomy is the most useful treatment for recurrent hepatocellular carcinoma. *J Hepatobiliary Pancreat Surg* 2001;**8**:410–6.
13. Kumada T, Nakano S, Takeda I, et al. Patterns of recurrence after initial treatment in patients with small hepatocellular carcinoma. *Hepatology* 1997;**25**:87–92.
14. Shimada M, Hamatsu T, Yamashita Y, et al. Characteristics of multicentric hepatocellular carcinomas: Comparison with intrahepatic metastasis. *World J. Surg.* 2001;**25**:991–5.
15. Hussein MR, Hassan M, Wood GS. Morphological changes and apoptosis in radial growth phase melanoma cell lines following ultraviolet-B irradiation. *Am J Dermatopathol* 2003;**25**:466–72.
16. Karachristos A, Liloglou T, Field JK, Deligiorgi E, Kouskouni E, Spandidos DA. Microsatellite instability and p53 mutations in hepatocellular carcinoma. *Mol Cell Biol Res Commun* 1999;**2**:155–61.
17. Scherer SJ, Welter C, Zang KD, Dooley S. Specific in vitro binding of p53 to the promoter region of the human mismatch repair gene hMSH2. *Biochem Biophys Res Commun* 1996;**221**:722–8.
18. Warnick CT, Dabbas B, Ford CD, Strait KA. Identification of a p53 response element in the promoter region of the hMSH2 gene required for expression in A2780 ovarian cancer cells. *J Biol Chem* 2001;**276**:27363–70.
19. Edmondson HA, Steiner PE. Primary carcinoma of the liver. A study of 100 cases among 48,900 necropsies. *Cancer* 1954;**7**:462–503.
20. Orita M, Suzuki Y, Sekiya T, Hayashi K. Rapid and sensitive detection of point mutation and DNA polymorphisms using the polymerase chain reaction. *Genomics* 1989;**5**:874–9.
21. Oda T, Tsuda H, Scarpa A, Skakmoto M, Hirohashi S. p53 gene mutation spectrum in hepatocellular carcinoma. *Cancer Res* 1992;**52**:6358–64.
22. Kobayashi K, Matsushima M, Koi S, et al. Mutational analysis of mismatch repair genes, hMLH1 and hMSH2, in sporadic endometrial carcinomas with microsatellite instability. *Jpn J Cancer Res* 1996;**87**:141–5.

23. Bhattacharyya NP, Skandalis A, Ganesh A, Groden J, Meuth M. Mutator phenotypes in human colorectal carcinoma cell lines. *Proc Natl Acad Sci USA* 1994;**91**:6319–23.
24. Hanford MG, Rushton BC, Gowen LC, Farber RA. Microsatellite mutation rates in cancer cell lines deficient or proficient in mismatch repair. *Oncogene* 1998;**16**:2389–93.
25. Wind N, Dekker M, Berns A, Radman M, Riele H. Inactivation of the mouse Msh2 gene results in mismatch repair deficiency, methylation torelance, hyperrecombination, and predisposition to cancer. *Cell* 1995;**82**:321–30.
26. Surtees JA, Argueso JL, Alani E. Mismatch repair proteins: key regulators of genetic recombination. *Cytogenet Genome Res* 2004;**107**:146–59.
27. Chan KT, Lung ML. Mutant p53 expression enhances drug resistance in a hepatocellular carcinoma cell line. *Cancer Chemother Pharmacol* 2004;**53**:519–26.
28. Rellecke P, Kuchelmeister K, Schachenmayr W, Schlegel J. Mismatch repair protein hMSH2 in primary drug resistance in in vitro human malignant gliomas. *J Neurosurg* 2004;**101**:653–8.
29. Lin X, Howell SB. DNA mismatch repair and p53 function are major determinants of the rate of development of cisplatin resistance. *Mol Cancer Ther* 2006;**5**:1239–47.
30. Liver Cancer Study Group of Japan. Classification of Primary Liver Cancer. Tokyo: Kanehara; 1997, p.38.
31. Yamamoto T, Kajino K, Kudo M, Sasaki Y, Arakawa Y, Hino O. Determination of the clonal origin of multiple human hepatocellular carcinomas by cloning and polymerase chain reaction of the integrated hepatitis B virus DNA. *Hepatology* 1999;**29**:1446–52.
32. Ng IO, Guan XY, Poon RT, Fan ST, Lee JM. Determination of the molecular relationship between multiple tumor nodules in hepatocellular carcinoma differentiates multicentric origin from intrahepatic metastasis. *J Pathol* 2003;**199**:345–53.
33. Morimoto O, Nagano H, Sakon M, et al. Diagnosis of intrahepatic metastasis and multicentric carcinogenesis by microsatellite loss of heterozygosity in patients with multiple and recurrent hepatocellular carcinomas. *J Hepatol* 2003;**39**:215–21.

Single nucleotide polymorphism in the *RAD18* gene and risk of colorectal cancer in the Japanese population

HIROTAKA KANZAKI[1], MAMORU OUCHIDA[1], HIROKO HANAFUSA[1], AKIKO SAKAI[1], HIROMASA YAMAMOTO[2], HIROMITSU SUZUKI[2], MASAAKI YANO[2], MOTOI AOE[2], KAZUE IMAI[3], HIROSHI DATE[2], KEI NAKACHI[3] and KENJI SHIMIZU[1]

[1]Department of Molecular Genetics and [2]Department of Cancer and Thoracic Surgery, Graduate School of Medicine, Dentistry and Pharmaceutical Sciences, Okayama University, Okayama 700-8558; [3]Department of Radiobiology/ Molecular Epidemiology, Radiation Effects Research Foundation, Hiroshima 732-0815, Japan

Received June 5, 2007; Accepted July 30, 2007

Abstract. The *RAD18* gene, located on the human chromosome 3p24-p25, plays a crucial role in post-replication repair (PRR) in various organisms from yeast to humans. In the human *RAD18* gene, one coding single nucleotide polymorphism (SNP) at codon 302, encoding either arginine (Arg, CGA) or glutamine (Gln, CAA), was reported. Although the molecular function of the RAD18 protein came to be elucidated, the association between the RAD18 Arg302Gln polymorphism and the risk of human cancer development was not examined. Therefore, we investigated the relationship between the polymorphism and the development of human primary colorectal cancer (CRC). The Arg302Gln polymorphism in 100 patients with CRC and 200 healthy controls were genotyped by the polymerase chain reaction with confronting two-pair primer (PCR-CTPP) assay. The Gln/Gln genotype was significantly more frequent in CRC (18.0%) than in the healthy controls (11.5%) (p=0.046). The increased risk was detected in CRC patients with the Gln/Gln genotype (Odds ratio [OR], 2.10; 95% confidence interval [CI], 1.00 to 4.40). When the relationship of the SNP with clinicopathological parameters of CRC was investigated, particularly in the well-differentiated grade and in the lymph node metastasis (N1) CRC patients, significantly higher risks were detected (OR, 7.00; 95% CI, 1.19-41.1 and OR, 3.71; 95% CI, 1.30-10.6, respectively). These results suggested that the RAD18 Arg302Gln polymorphism is associated with the risk of CRC. This report provides evidence for an association between the RAD18 Arg302Gln polymorphism and human CRC risk.

Correspondence to: Dr Mamoru Ouchida, Department of Molecular Genetics, Graduate School of Medicine, Dentistry and Pharmaceutical Sciences, Okayama University, 2-5-1 Shikata-cho, Okayama 700-8558, Japan
E-mail: ouchidam@md.okayama-u.ac.jp

Key words: single nucleotide polymorphism, RAD18, post-replication repair, colorectal cancer, cancer predisposition

Introduction

Any DNA damage induced by mutagens, such as UV light and mutagenic chemicals, must be repaired by DNA repair systems (1). However, when the DNA repair systems are stalled or saturated and such DNA damage is therefore not removed before the onset of DNA replication, single-stranded gaps are generated. These gaps will be filled by the post-replication repair (PRR) system. The molecular mechanisms of PRR are less clearly elucidated in comparison to the other repair pathways. The RAD6 pathway is known to be central to PRR (2). The genes belonging to the *RAD6* epistasis group, such as the *RAD5*, *RAD18*, *RAD30*, *MMS2* and *UBC13* genes, are all involved in the pathway. Among these gene products, RAD6 and RAD18 are two of the most important proteins and play a central role in this pathway. RAD6 is a ubiquitin-conjugating enzyme (E2) in the proteasome protein degradation system (3-5). RAD6 forms a tight complex with RAD18 (6-8), which is a single-strand DNA binding protein with a RING-finger domain (9) and ubiquitin-ligating enzymes (E3). Although RAD6 interacts with several E3, the interaction with RAD18 is essential for carrying out PRR (5,6,10,11). Since RAD6 interacts tightly with RAD18, although RAD6 does not have any DNA binding activity, it is proposed that RAD18 recruits RAD6 to the site of DNA damage via its physical interaction, where RAD6 and its complex then modulate stalled DNA replication through their ubiquitin-conjugating activity. There are reports that the proliferating cell nuclear antigen (PCNA), a DNA polymerase sliding clamp that is involved in DNA synthesis and repair, is a substrate of the ubiquitin-conjugating enzyme and it is ubiquitinated in a RAD6- and RAD18-dependent manner. Therefore, the monoubiquitination of PCNA through RAD6 and RAD18 is necessary for carrying out DNA PRR (12-16).

It was also reported that RAD18 knockout cells of mouse embryonic stem cells (17) and of chicken DT40 cells (18) were hypersensitive to various DNA-damaging agents and showed

defective PRR. These cells also showed genomic instability demonstrated by increased rates of the sister chromatid exchange and integration of the exogenous DNA (17,18). Therefore, the dysfunction of RAD18 increases the frequency of homologous recombination and illegitimate recombination and RAD18 contributes to the maintenance of genomic stability through PRR (19). The dysfunction of RAD18 is also thought to lead to the development of cancer (1,20).

The genetic polymorphisms of DNA repair genes were analyzed to determine the susceptibility to several cancers, including lung (21,22), colorectal (23), head and neck (24), breast (25), bladder cancer (26) and leukemia (27). The *RAD18* gene is known to have a single nucleotide polymorphism (SNP) at codon 302, encoding either arginine (CGA) or glutamine (CAA), while the function of this SNP and its molecular mechanism is not clarified. We conducted a pilot study to see whether the RAD18 Arg302Gln polymorphism is associated with cancer-incidence and found a significant correlation with CRC. This report provides evidence for an association between the RAD18 Arg302Gln polymorphism and human CRC risk.

Table I. Characteristics of CRC patients and healthy controls.

	Patients n (%) (n=100)	Controls n (%) (n=200)	p-value
Gender			0.371
Male	61 (61.0)	133 (66.5)	
Female	39 (39.0)	67 (33.5)	
Age (years ± SD)	65.1±10.1	65.6±9.42	
Smoking habit			0.052[a]
No-smoker	42 (42.0)	63 (31.5)	
Smoker	55 (55.0)	137 (68.5)	
<20 pack-years	14 (25.5)	17 (12.4)	
≥20 pack-years	40 (72.7)	87 (63.5)	
Unknown	1 (1.8)	33 (24.1)	
Unknown	3 (3.0)	0 (0.0)	

The mean age of each group with a standard deviation is shown. [a]p-values are for the differences in the number of smokers and non-smokers between the patients and the controls.

Materials and methods

Subjects. We analyzed 100 Japanese patients chosen from those who were histologically diagnosed as having primary colorectal cancer and who underwent surgical operation at Okayama University Hospital (Okayama, Japan) in 1994-2003. Patients were gathered not only from Okayama but also from 10 other prefectures in Western Japan, mainly the Chugoku and Shikoku Districts (around Okayama). We confirmed that all CRC patients have primary colorectal carcinomas by microscope. Clinical stage and pathological grade in all CRC patients were confirmed by operation and pathology. The clinicopathological staging and histological classification were according to the criteria of the UICC Tumor-Node-Metastasis Classification of Malignant Tumor (TNM), 6th edition, 2002, colon and rectum (ICD-O C18-C20). For the controls, each of the 200 healthy controls we analyzed were selected by computer-aided randomization, all of which were from the subjects of cohort studies on a Japanese general population >40 years of age in a town near the Saitama Cancer Center. The residents in this town are neither genetically nor demographically close, *i.e.*, its population increased because of a population influx from other areas, with a social increase rate of about 5% every year for 15 years. Written informed consent was obtained from all of the cancer patients and controls concerned. This study was approved by The Bioethics Committee of Okayama University Medical School. The characteristics of the 100 CRC patients and the 200 controls are shown in Table I. There were no significant differences in gender and age at recruitment between the CRC patients and the controls ($p \geq 0.05$). Pack-year equivalents [(cigarettes/day/20) x (smoking years)] were used for smoking status (we could not obtain smoking status for 3 out of the 100 patients).

DNA extraction. The genomic DNA of cancer patients was isolated from the non-cancerous region of the resected specimens or from the mononuclear cells of the peripheral blood by the standard method of proteinase K digestion and phenolchloroform extraction. The genomic DNA of the healthy controls was extracted from the peripheral lymphocytes.

Genetic analysis. The RAD18 Arg302Gln polymorphism was detected by polymerase chain reaction using the confronting two-pair primer (PCR-CTPP) method (28,29). According to the published sequence of the human *RAD18* gene, we designed two sets of paired primers. The first set of primers was as follows: forward primer 1, 5'-ATA CCC ATC ACC CAT CTT C-3' and reverse primer 1, 5'-GTC TTC TCT ATA TTT TCG ATT TCT T-3' for the Gln allele amplifying a 146-bp band. The second set of primers was as follows: forward primer 2, 5'-TTA ACA GCT GCT GAA ATA GTT CG-3' and reverse primer 2, 5'-CTG AAA TAG CCC ATT AAC ATA CA-3' for the Arg allele amplifying a 106-bp band. A 206-bp band was designed between the forward primer 1 and the reverse primer 2. The reaction mixture (20 μl) contained 40 μM of each dNTP, 1X PCR buffer, 8 pmol of the forward primer 1 and reverse primer 2, 24 pmol of the forward primer 2 and reverse primer 1, 20 ng of the genomic DNA and 0.5 units of the Taq DNA polymerase (Takara, Kyoto, Japan). The PCR amplification was initiated by a denaturing step at 94°C for 3 min, followed by 35 cycles at 94°C for 30 sec, 64°C for 1 min, 72°C for 1 min and a final extension step at 72°C for 7 min. For genotyping, the PCR products were subjected to electrophoresis in 3% agarose gel, stained with ethidium bromide and then visualized on a UV trans-illuminator. In order to confirm the allele types, certain PCR products were processed with the Big Dye terminator Cycle Sequencing Kit (Applied Biosystems, Foster City, CA, USA), then analyzed and confirmed on an ABI 3100 sequencer (Applied Biosystems).

Statistical analysis. We compared the allele frequencies of the Arg/Gln (CGA/CAA) polymorphism in the *RAD18* gene between the healthy control group and the patient groups with

CRC. The distribution of the *RAD18* genotype (Arg/Arg, Arg/Gln, Gln/Gln) in all of the patients and the controls was tested for adherence to the Hardy-Weinberg equilibrium. The statistical analyses were conducted by the SPSS software Ver.12.0 (SPSS Inc., Tokyo, Japan). The Chi-square test was used to compare the genotype distribution between the cancer patients and the healthy controls. The odds ratio (OR) and 95% confidence interval (95% CI) were both adjusted for age, gender and smoking status using an unconditional logistic regression model. The relationship between the genotype and the clinicopathological parameters was examined by the Chi-square test and Fisher's exact probability test. A p-value of <0.05 was considered to be statistically significant.

Results

Assessment of cancer risk by RAD18 genotyping. The characteristics of the 100 CRC patients and the 200 healthy controls are shown in Table I. There were no significant differences in gender, age or smoking status between the two groups. Pack-year equivalents were used for smoking status (however, we could not obtain the smoking status for 3 out of the 100 CRC patients).

Fig. 1A shows a representative polymerase chain reaction with confronting two pair primer (PCR-CTPP) assay patterns of the Arg/Gln (CGA/CAA) genotypes in the codon 302 of the RAD18 gene. The allele types were determined as follows: two fragments of 205- and 106-bp for the Arg/Arg (G/G) genotype, two fragments of 205- and 146-bp for the Gln/Gln (A/A) genotype and three fragments of 205-, 146- and 106-bp for the Arg/Gln (G/A) genotype. We confirmed that each PCR mixture contained no non-specific bands by electrophoresis in 3% agarose gel. The genotypes were confirmed by the subsequent sequencing of representative cases (Fig. 1B).

The genotype analysis of this SNP revealed that the genotype frequency was significantly different between the control and patient groups. The frequencies of the three genotypes in the *RAD18* gene are shown in Table II. The frequencies of the genotypes Arg/Arg, Arg/Gln and Gln/Gln found were 43.0, 45.5 and 11.5% in the controls and 32.0, 50.0 and 18.0% in the CRC patients. All of the results fitted the Hardy-Weinberg equilibrium. Compared to the controls with the Arg/Arg genotype, CRC patients with the homozygous Gln/Gln genotype exhibited the most significantly increased risk with an odds ratio (OR) of 2.10 (95%CI, 1.00-4.40), therefore suggesting that the homozygous Gln/Gln (A/A) genotype has an enhanced risk of CRC development.

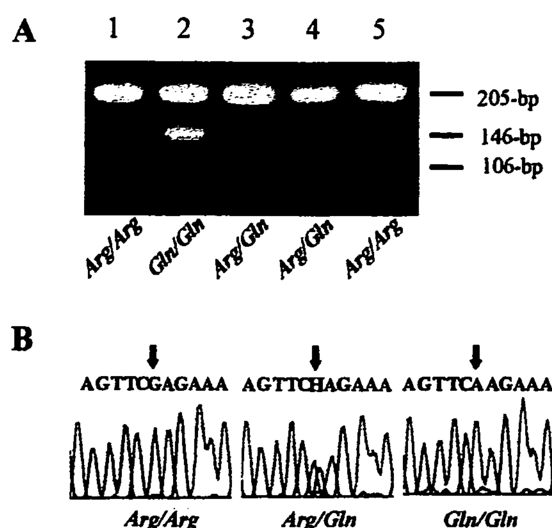

Figure 1. The single nucleotide polymorphism of the *RAD18* gene at codon 302. (A) The PCR-CTPP patterns of the *RAD18* SNP. The PCR product was electrophoresed in 3% agarose gel. Two fragments of 205- and 106-bp show the Arg/Arg (G/G) genotype, two fragments of 205- and 146-bp show the Gln/Gln (A/A) genotype and three fragments of 205-, 146- and 106-bp show the Arg/Gln (G/A) genotype. The case number and genotypes are shown at the top and bottom, respectively. (B) DNA sequence patterns of the *RAD18* SNP. Heterozygous signals (G/A) are shown by arrows in the Arg/Gln genotype.

The association between the RAD18 genotype and clinicopathological parameters in CRC patients. When we analyzed the relationship between the genotype distribution and the clinicopathological parameters of the CRC patient group, the well-differentiated grade and lymph node metastasis (N1) patients with the A/A genotype exhibited a significantly increased risk with an adjusted OR of 7.00 (95% CI=1.19-41.1) and 3.71 (95%CI=1.30-10.6), respectively (Table III). There were no overall differences in genotype distribution within each parameter using the Chi-square test or the

Table II. The RAD18 genotypes in CRC patients and healthy controls.

RAD18 genotype	Patients n (%)	Controls n (%)	p-value	OR (95% CI)
Arg/Arg	32 (32.0)	86 (43.0)		Ref. 1
Arg/Gln	50 (50.0)	91 (45.5)	0.151[a]	1.47 (0.87-2.52)
Gln/Gln	18 (18.0)	23 (11.5)	0.046[a]	2.10 (1.00-4.40)
Total	100	200		
Allele frequencies			0.037	
Arg	114 (57.0)	263 (67.8)		
Gln	86 (43.0)	137 (34.2)		

[a]p-values are shown against Arg/Arg genotype between patients and controls.

Table III. Association between the RAD18 genotype and clinicopathological parameters of CRC patients.

	Genotype (%)					OR[b] (95%CI)	
Characteristics	Arg/Arg	Arg/Gln	Gln/Gln	Total	p-value[a]	Arg/Gln	Gln/Gln
Differentiated grade					0.172		
Well	2 (11.1)	11 (61.1)	5 (27.8)	18		4.71 (1.00-22.2)	7.00 (1.19-41.1)
Moderate	25 (33.8)	36 (48.6)	13 (17.6)	74		1.31 (0.72-2.39)	1.68 (0.72-3.89)
Poor	2 (66.7)	1 (33.3)	0 (0.0)	3		NE	NE
Others	3 (60.0)	2 (40.0)	0 (0.0)	5			
T					0.007		
Tis, T1, T2	0 (0.0)	10 (71.4)	4 (28.6)	14		NE	NE
T3, T4	32 (37.2)	40 (46.5)	14 (16.3)	86		1.14 (0.65-2.00)	1.32 (0.58-3.00)
N					0.097		
N0	13 (28.9)	24 (53.3)	8 (17.8)	45		1.55 (0.73-3.31)	1.82 (0.63-5.18)
N1	9 (25.0)	18 (50.0)	9 (25.0)	36		1.91 (0.81-4.51)	3.71 (1.30-10.6)
N2	9 (56.3)	7 (43.7)	0 (0.0)	16		0.75 (0.27-2.10)	NE
Unknown	1 (33.3)	1 (33.3)	1 (33.3)	3			
M					0.622		
M0	20 (29.9)	34 (50.7)	13 (19.4)	67		1.59 (0.84-3.01)	2.22 (0.93-5.33)
M1	12 (38.7)	15 (48.4)	4 (12.9)	31		1.18 (0.52-2.70)	1.19 (0.35-4.10)
Unknown	0 (0.0)	1 (50.0)	1 (50.0)	2			
TNM stage					0.929		
0.I.II	12 (30.8)	20 (51.3)	7 (17.9)	39		1.47 (0.66-3.26)	1.66 (0.55-5.02)
III.IV	20 (34.5)	28 (48.3)	10 (17.2)	58		1.35 (0.71-2.60)	1.84 (0.75-4.53)
Unknown	0 (0.0)	2 (66.7)	1 (33.3)	3			

[a]p-values were calculated by the Chi-square test or the Fisher's exact test. [b]ORs were adjusted for age, gender and smoking status. The Arg/Arg genotype was defined as the reference. T, primary tumor; N, lymph node metastasis; M, distant metastasis; NE, not estimated.

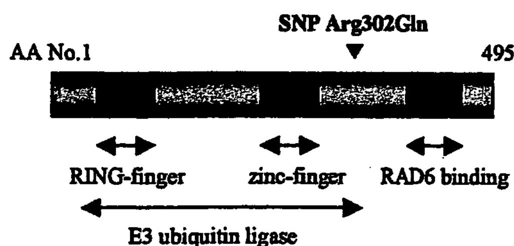

Figure 2. The location of the polymorphism and the functional motifs of RAD18. The SNP (Arg302Gln) is indicated by an arrowhead above the motif. The motifs of the RAD18 protein are depicted in dark gray and/or by arrows. The RING-finger, a really interesting new gene domain (AA25-63); zinc-finger, zinc-finger motif (AA201-223); RAD6 binding, RAD6 binding domain (AA371-410); E3 ubiquitin ligase, RING-finger-containing E3 ubiquitin-ligase domain (AA16-304). AA No., amino acid number.

Fisher's exact test, while the genotype distribution in the tumor stages may be biased due to the small sample size.

Discussion

In this study, we examined whether an SNP (Arg302Gln) in the *RAD18* gene is associated with the risk for the development, progression and metastasis of CRC. We found significant differences in the genotype distribution between the CRC patients and the healthy controls. Our findings suggest that the Gln allele enhance the susceptibility to the development of CRC (p=0.046, OR=2.10). We also found a significant association between polymorphism and clinicopathological features, specifically in differentiated grade and lymph node metastasis. The Gln allele was detected more frequently in patients with well-differentiated grade and lymph node metastasis (N1) (OR=7.00 and 3.71, respectively). These data also suggest that this SNP may become a prognostic marker. Our findings suggest an association between the RAD18 Arg302Gln polymorphism and the risk of CRC. No other studies have found any association between human cancers and the RAD18 SNPs.

Although the molecular mechanism of the association between this SNP and cancer development is not yet clarified, several of the functions and functional domains of RAD18 were revealed. RAD18 is one of the most important proteins involved in the PRR pathway. While a number of proteins are known to be involved in the PRR pathway and RAD18 interacts with several of these proteins, the interaction with RAD6 in particular is essential for carrying out PRR (5,6,10,11). RAD18 interacts with RAD6 through the RAD6 binding domain in the C-terminal region (Fig. 2). RAD18 has several other functional domains, such as the RING-finger

motif (25), zinc-finger motif (30,31) and E3 ubiquitin-ligase domain. The RING-finger motif, residing in the N-terminal region and the E3 ubiquitin-ligase domain together confer an ubiquitin-ligase activity on RAD18. The middle part of RAD18 contains a zinc-finger motif, which is considered to mediate protein-to-protein interaction or DNA binding. The RAD18 Arg302Gln polymorphism is located in the E3 ubiquitin-ligase domain (Fig. 2). Therefore, this SNP may affect the activity of RAD18, especially the ubiquitin-ligase activity. It is also possible that this SNP may affect the interaction between RAD18 and other proteins involved in PRR through its structural change, which is generated by the substitution of one amino acid residue, a basic amino acid residue (Arg), to a neutral residue (Gln). Considering that the Gln/Gln genotype was much more frequently found in the CRC patients than in the controls, the RAD18 with the Gln genotype may have decreased PRR activity and consequently may affect cancer development and progression.

In conclusion, our data provide evidence for an association between the RAD18 Arg302Gln polymorphism and the risk for the development and progression of CRC. It is possible that this polymorphism may influence susceptibility to a variety of human cancers through incomplete PRR. Further study with sufficiently larger populations and functional analysis of this polymorphism is needed in order to clarify this issue. Although the sample size we analyzed was small, the findings of this study are statistically significant. We expect that this study may contribute to the development of a novel strategy for the early diagnosis and prevention of CRC.

Acknowledgements

We thank the members of our University Hospital for their cooperation in specimen-sampling. This study was supported by a Grant-in-Aid for Scientific Research on Priority Area (No.12213084) to KS from the Ministry of Education, Culture, Sports, Science and Technology of Japan.

References

1. Hoeijmakers JH: Genome maintenance mechanisms for preventing cancer. Nature 411: 366-374, 2001.
2. Lawrence C: The RAD6 DNA repair pathway in Saccharomyces cerevisiae: what does it do, and how does it do it? Bioessays 16: 253-258, 1994.
3. Sung P, Prakash S and Prakash L: Mutation of cysteine-88 in the Saccharomyces cerevisiae RAD6 protein abolishes its ubiquitin-conjugating activity and its various biological functions. Proc Natl Acad Sci USA 87: 2695-2699, 1990.
4. Sung P, Prakash S and Prakash L: Stable ester conjugate between the Saccharomyces cerevisiae RAD6 protein and ubiquitin has no biological activity. J Mol Biol 221: 745-749, 1991.
5. Wood A, Schneider J, Dover J, Johnston M and Shilatifard A: The Paf1 complex is essential for histone monoubiquitination by the Rad6-Bre1 complex, which signals for histone methylation by COMPASS and Dot1p. J Biol Chem 278: 34739-34742, 2003.
6. Bailly V, Lamb J, Sunq P, Prakash S and Prakash L: Specific complex formation between yeast RAD6 and RAD18 proteins: a potential mechanism for targeting RAD6 ubiquitin-conjugating activity to DNA damage sites. Genes Dev 8: 811-820, 1994.
7. Bailly V, Lauder S, Prakash S and Prakash L: Yeast DNA repair proteins Rad6 and Rad18 form a heterodimer that has ubiquitin-conjugating, DNA binding and ATP hydrolytic activities. J Biol Chem 272: 23360-23365, 1997.
8. Bailly V, Prakash S and Prakash L: Domains required for dimerization of yeast Rad6 ubiquitin-conjugating enzyme and Rad18 DNA binding protein. Mol Cell Biol 17: 4536-4543, 1997.
9. Joazeiro CA and Weissman AM: RING-finger proteins: mediators of ubiquitin-ligase activity. Cell 102: 549-552, 2000.
10. Dohmen RJ, Madura K, Bartel B and Varshavsky A: The N-end rule is mediated by the UBC2 (RAD6) ubiquitin-conjugating enzyme. Proc Natl Acad Sci USA 88: 7351-7355, 1991.
11. Sung P, Berleth E, Pickart C, Prakash S and Prakash L: Yeast RAD6 encoded ubiquitin conjugating enzyme mediates protein degradation dependent on the N-end-recognizing E3 enzyme. EMBO J 10: 2187-2193, 1991.
12. Haracska L, Torres-Ramos CA, Johnson RE, Prakash S and Prakash L: Opposing effects of ubiquitin conjugation and SUMO modification of PCNA on replicational bypass of DNA lesions in Saccharomyces cerevisiae. Mol Cell Biol 24: 4267-4274, 2004.
13. Hoege C, Pfander B, Moldovan GL, Pyrowolakis G and Jentsch S: RAD6-dependent DNA repair is linked to modification of PCNA by ubiquitin and SUMO. Nature 419: 135-141, 2002.
14. Stelter P and Ulrich HD: Control of spontaneous and damage-induced mutagenesis by SUMO and ubiquitin conjugation. Nature 425: 188-191, 2003.
15. Kannouche PL, Wing J and Lehmann AR: Interaction of human DNA polymerase eta with monoubiquitinated PCNA: a possible mechanism for the polymerase switch in response to DNA damage. Mol Cell 14: 491-500, 2004.
16. Watanabe K, Tateishi S, Kawasuji M, Tsurimoto T, Inoue H and Yamaizumi M: Rad18 guides poleta to replication stalling sites through physical interaction and PCNA monoubiquitination. EMBO J 23: 3886-3896, 2004.
17. Tateishi S, Niwa H, Miyazaki J, Fujimoto S, Inoue H and Yamaizumi M: Enhanced genomic instability and defective post-replication repair in RAD18 knockout mouse embryonic stem cells. Mol Cell Biol 23: 474-481, 2003.
18. Yamashita YM, Okada T, Matsusaka T, *et al*: RAD18 and RAD54 cooperatively contribute to maintenance of genomic stability in vertebrate cells. EMBO J 21: 5558-5566, 2002.
19. Shekhar MP, Lyakhovich A, Visscher DW, Heng H and Kondrat N: Rad6 overexpression induces multinucleation, centrosome amplification, abnormal mitosis, aneuploidy and transformation. Cancer Res 62: 2115-2124, 2002.
20. Friedberg EC: DNA damage and repair. Nature 421: 436-440, 2003.
21. Ryk C, Kumar R, Thirumaran RK and Hou SM: Polymorphisms in the DNA repair genes XRCC1, APEX1, XRCC3 and NBS1 and the risk for lung cancer in never- and ever-smokers. Lung Cancer 54: 285-292, 2006.
22. Ito H, Matsuo K, Hamajima N, *et al*: Gene-environment interactions between the smoking habit and polymorphisms in the DNA repair genes, APE1 Asp148Glu and XRCC1 Arg399Gln, in Japanese lung cancer risk. Carcinogenesis 25: 1395-1401, 2004.
23. Yamamoto H, Hanafusa H, Ouchida M, *et al*: Single nucleotide polymorphisms in the EXO1 gene and the risk of colorectal cancer in a Japanese population. Carcinogenesis 26: 411-416, 2005.
24. Huang WY, Olshan AF, Schwartz SM, *et al*: Selected genetic polymorphisms in MGMT, XRCC1, XPD and XRCC3 and risk of head and neck cancer: a pooled analysis. Cancer Epidemiol Biomarkers Prev 14: 1747-1753, 2005.
25. Costa S, Pinto D, Pereira D, *et al*: DNA repair polymorphisms may contribute differentially on familial and sporadic breast cancer susceptibility: a study on a Portuguese population. Breast Cancer Res Treat 103: 209-217, 2007.
26. Zhu Y, Lai M, Yang H *et al*: Genotypes, haplotypes and diplotypes of XPC and risk of bladder cancer. Carcinogenesis 28: 698-703, 2007.
27. Bolufer P, Barragan E, Collado M, Cervera J, López JA and Sanz MA: Influence of genetic polymorphisms on the risk of developing leukemia and on disease progression. Leuk Res 30: 1471-1491, 2006.
28. Hamajima N: PCR-CTPP: a new genotyping technique in the era of genetic epidemiology. Expert Rev Mol Diagn 1: 119-123, 2001.
29. Hamajima N, Saito T, Matsuo K, Kozaki K, Takahashi T and Tajima K: Polymerase chain reaction with confronting two-pair primers for polymorphism genotyping. Jpn J Cancer Res 91: 865-868, 2000.
30. Mackay JP and Crossley M: Zinc fingers are sticking together. Trends Biochem Sci 23: 1-4, 1998.
31. Akhtar A and Becker PB: The histone H4 acetyltransferase MOF uses a C2HC zinc finger for substrate recognition. EMBO Rep 2: 113-118, 2001.

ELSEVIER

Available online at www.sciencedirect.com

ScienceDirect

Journal of Steroid Biochemistry & Molecular Biology 105 (2007) 106–114

The Journal of Steroid Biochemistry & Molecular Biology

www.elsevier.com/locate/jsbmb

Demethylation of promoter C region of estrogen receptor α gene is correlated with its enhanced expression in estrogen-ablation resistant MCF-7 cells

Tetsuya Sogon [a,b], Shigeru Masamura [c], Shin-ichi Hayashi [d], Richard J. Santen [e], Kei Nakachi [a,b], Hidetaka Eguchi [a,b,*]

[a] *Department of Molecular Epidemiology, Hiroshima University Graduate School of Biomedical Sciences, Radiation Effects Research Foundation, 5-2, Hijiyama-park, Minami-ku, Hiroshima 732-0815, Japan*

[b] *Department of Radiobiology/Molecular Epidemiology, Radiation Effects Research Foundation, 5-2, Hijiyama-park, Minami-ku, Hiroshima 732-0815, Japan*

[c] *Department of Surgery, Tokyo Dental College Ichikawa General Hospital, 5-11-13, Sugano, Ichikawa, Chiba 272-8513, Japan*

[d] *Department of Medical Technology, Tohoku University School of Medicine, 2-1, Seiryocho, Aoba-ku, Sendai 980-8575, Japan*

[e] *University of Virginia Health System, Charlottesville, VA 22908, USA*

Received 7 July 2006; accepted 29 December 2006

Abstract

Long-term estrogen deprivation (LTED) MCF-7 cells showing estrogen-independent growth, express estrogen receptor (ER) α at a much higher level than wild-type MCF-7 cells. Enhanced expression of ERα associated with partial localization of ERα to the plasma membranes in LTED cells is thought to be an important step for acquisition of estrogen-ablation resistance. In this study, we compared the regulation of ERα gene expression between wild type and LTED cells, examining the usage of the promoters A and C as well as their methylation status. We found that transcription from the promoter C was drastically enhanced in LTED cells, compared with that in wild-type cells. Furthermore, the promoter C region was highly unmethylated in LTED cells, but partially methylated in wild-type cells. Our findings imply that demethylation of promoter C region in the ERα gene is in part responsible for the enhanced expression of ERα gene in LTED cells.
© 2007 Elsevier Ltd. All rights reserved.

Keywords: Estrogen receptor α; Breast cancer; Methylation

1. Introduction

Experimental, clinical, and epidemiologic data suggest that estrogens contribute to the development of breast cancer. Estrogens bind to ERα or β and stimulate the transcription of target genes involved in cell proliferation. Thus, the anti-estrogen therapy such as tamoxifen has been generally used for ERα-positive breast cancer for several decades. Recently, clinical trials in the adjuvant, neoadjuvant and advanced disease setting have demonstrated a greater clinical efficacy of the aromatase inhibitors aiming to decrease the concentration of estrogen, compared with selective estrogen receptor modulators represented by tamoxifen [1,2]. On the other hand, clinical observations suggested that some human breast cancers adapted to hormone-ablative therapy involving surgically deprivation of estrogen production. Hormone-dependent breast cancers often regress in response to surgical removal of the ovaries, a treatment which lower circulating plasma estradiol (E2) from approximately 200–15 pg/ml [3]. In response to this acute deprivation of E2, tumors regress for 12–18 months on average before they begin to regrow. Second-line therapy with surgical oophorectomy or with aromatase inhibitors can then induce additional tumor regression by lowering E2 concentrations further to 1–5 pg/ml [4]. These

* Corresponding author at: Department of Radiobiology/Molecular Epidemiology, Radiation Effects Research Foundation, 5-2, Hijiyama-park, Minami-ku, Hiroshima 732-0815, Japan. Tel.: +81 82 261 3169; fax: +81 82 261 3170.

E-mail address: eguchi@rerf.or.jp (H. Eguchi).

0960-0760/$ – see front matter © 2007 Elsevier Ltd. All rights reserved.
doi:10.1016/j.jsbmb.2006.12.104

observations for the first time demonstrated enhanced sensitivity to circulating E2.

In order to demonstrate the phenomenon of adaptive hypersensitivity and to determine the mechanisms involved, we have established a model system involving MCF-7 human breast cancer cells *in vitro*. Wild-type MCF-7 cells were cultured over a prolonged period in estrogen-free medium to mimic the effect of ablative endocrine therapy such as induced by surgical oophorectomy [5]. This process involves long-term E2 deprivation; the adapted cells are called LTED cells. When LTED cells were cultured in the presence of E2 for 4 months, the cells showed estrogen-dependent growth as was observed for wild-type MCF-7 cells [5].

Importantly, ERα is expressed at a much higher level in LTED cells than in wild-type MCF-7 cells [6]. In concert with this observation, an elevated basal ER transactivation activity (mean increase; 5-fold) was measured in LTED cells compared with the wild-type cells using pERE-tk-CAT, a reporter gene driven by estrogen responsive element-thymidine kinase promoter [6].

In addition to the established role as a nuclear receptor, ERα may have another function on the plasma membrane. In LTED cells, ERα localizes predominantly to the nuclei and some also present on the plasma membranes [7]. The sub-cellular localization of ERα to the plasma membranes in LTED cells may, at least in part, be due to the enhanced expression of ERα in LTED cells, since plasma membrane-associated ERα can only be observed in ERα-enriched MCF-7 sub-cell lines (mER^{high}) but not ERα-depleted ones ($mER\alpha^{low}$) [8]. Constitutively activated MAP kinase activity was observed in LTED cells independent of serum factors [9]. A rapid physical interaction of the plasma membrane-associated ERα and an adaptor protein Shc has been observed upon addition of E2 [7]; Shc is subsequently phosphorylated and triggers the MAP kinase signaling pathway [10,11].

Thus, when ERα works as a transcription factor in the nuclei and also as a signal transducer on the plasma membranes, typically in LTED cells, enhanced expression of ERα may be an obligatory step for acquisition of estrogen-ablation resistance. Though, the mechanisms how ERα expresses at high level in LTED cells still remain unknown.

Several human ERα gene promoters (A–F) are identified so far [12]. These promoters are differently utilized in a tissue- and cell-dependent manner [13–15]. Among these promoters, we previously demonstrated that the transcript from promoter A was constitutively used in both normal and cancerous mammary tissue, while the transcript from promoter C (formerly called promoter B) showed remarkable correlation to the ERα protein levels in ERα-positive breast cancer [16]. Furthermore, we have identified a *cis*-acting element, ERBF-1, that plays an important role in the expression of the ERα gene transcribed from promoter C in breast cancer cells [17]. On the other hand, a transcription factor ERF-1, a member of AP2 transcription factor, is important for the transcriptional regulation of promoter A [18,19]. In addition, methylation of the promoter A and C regions was critical for the repression of gene transcription from these promoters [20]. Collectively, methylation of these promoter regions as well as alteration of critical transcription factors are thought to be important for ERα gene expression in breast cancer cells.

In this study, we examined regulation of ERα gene expression in wild-type MCF-7 and LTED cells. We first found that transcription from the promoter C was drastically enhanced in LTED cells, compared with that in the wild-type cells. Transient transfection with a reporter gene driven by the promoter A or promoter C of ERα gene revealed that transcription factors are equally available in these cells. Second, differences in epigenetic alterations of promoter C were found between LTED and wild-type cells: The promoter C region was highly unmethylated in LTED cells, while that in wild-type cells was partially methylated. Our findings imply that demethylation of promoter C region in the ERα gene is in part responsible for the enhanced expression of ERα gene in LTED cells.

2. Materials and methods

2.1. Tissue culture

Human breast cancer cells wild-type MCF-7 were maintained in improved MEM (IMEM) containing 5% dextran-coated charcoal-stripped fetal bovine serum (DCC-FBS) and 10 nM E2. LTED cells were established by long-term culture of wild-type MCF-7 cells in IMEM containing 5% DCC-FBS. The established LTED cells were stored in liquid nitrogen until use. LTED cells were maintained in IMEM containing 5% DCC-FBS.

2.2. Plasmid

Reporter plasmids pGL3-ProA 1.3K and pGL3-ProC (formerly called pGL3-ProB1.4K) were described previously [20]. An internal control pRL-TK was purchased from Promega (Madison, WI).

2.3. RNA extraction and cDNA synthesis

Total RNA was prepared from wild type and LTED cells using RNeasy Mini kit (QIAGEN, Hilden, Germany). One μg of total RNA was reverse transcribed with Quantitect Reverse Transcription (QIAGEN) using RT primer mix as primers in a final volume of 20 μl at 42 °C for 15 min.

2.4. Real-time PCR analysis of ERα mRNA expression

The real-time PCR was performed in triplicate using iCycler iQ (Bio-Rad Laboratories, Hercules, CA). Reaction mixture consisted of 1 μl of cDNA products, 0.2 μM of each primers and 12.5 μl of SYBR Green ROX Mix (ABgene, Epsom, UK) in a total volume of 25 μl. PCR thermal conditions were as following: 95 °C for 15 min for 1 cycle and 95 °C for 20 s, 60 °C for 15 s, 72 °C for 10 s, and 86 °C for

15 s (fluorescent signal collection) for 50 cycles for detection of ERα mRNA from promoters A and C; 95 °C for 15 min for 1 cycle and 94 °C for 15 s, 68 °C for 30 s, and 86 °C for 15 s (fluorescent signal collection) for 50 cycles for detection of total ERα mRNA. The following primers were used: PROA1, 5′-ACC TCG GGC TGT GCT CTT-3′ and PRODW, 5′-GAG GGT CAT GGT CAT GGT-3′ for ERα mRNA from promoter A; PROB3, 5′-GCC CAG GAA CAT TTC TGG AA-3′ and PRODW for ERα mRNA from promoter C; EREX1, 5′-AGA ACG AGC CCA GCG GCT AC-3′ and EREX2-R, 5′-CCT TGC AGC CCT CAC AGG AC-3′ for total ERα mRNA. For construction of standard curves, serially diluted plasmids harboring fragment of target gene sequences were used after digestion with *Not* I restriction enzyme to release the insert fragments. As a control, β-actin mRNA was also measured as described previously [21].

2.5. *Transient transfection assays*

A transient transfection of the plasmids was performed in triplicate using SuperFect Transfection Reagent (QIAGEN) under manufacturer's instruction. Briefly, 1×10^5 cells were plated onto 24 wells plastic dish. After over night culture, 1 μg of pGL3-ProA1.3K or pGL3-ProC and 0.1 μg of pRL-TK were mixed with 5 μl of the SuperFect Transfection Reagent in 350 μl of the medium with 5% DCC-FBS and subjected to transfection. After 2 h incubation, the medium was replaced with a fresh medium and cells were incubated for 48 h. Then, cells were collected and lysed using Passive Lysis Buffer (Promega). Luciferase assays were performed using Dual-Luciferase Reporter Assay System (Promega) and TD-20/20 Luminometer (TURNER DESIGNS, CA).

2.6. *Bisulfite modification and methylation-specific PCR*

Total DNA was extracted from wild type and LTED cells using NucleoSpin Tissue (MACHEREY-NAGEL, Düren, Germany). DNA was subjected to bisulfite conversion using EZ DNA Methylation kit (ZYMO Research, Orange, CA) according to the manufacture's instruction, essentially based on the report by Herman et al. [22]. Briefly, after denaturation with NaOH, 500 ng of DNA was incubated in a buffer containing sodium bisulfite at 50 °C for 16 h, followed by purification using ZYMO-Spin I column. Bisulfite-converted DNA was eluted in 10 μl of M-Elution buffer. First PCR amplification aiming to amplify bisulfite-converted DNA fragments was performed in 20 μl of reaction mixture containing 1 μl of bisulfite-treated genomic DNA, 0.5 μM each primers, 0.2 mM dNTPs, 2.5 mM $MgCl_2$ and 1.25 units of AmpliTaq Gold DNA polymerase (Applied Biosystem, Foster, CA) under the following conditions: 95 °C for 5 min for 1 cycle and 95 °C for 15 s, 54 °C for 15 s, and 72 °C for 1 min for 35 cycles. Second PCR amplification using methylation- or unmethylation-specific primers was performed in 20 μl of reaction mixture containing 1 μl of first PCR product (1/100 diluted with MilliQ water), 0.5 μM each primers, 0.2 mM dNTPs, 2.5 mM $MgCl_2$ and 1.25 units of AmpliTaq Gold DNA polymerase under the following conditions: 95 °C for 5 min for 1 cycle and 95 °C for 15 s, 57 °C (methylation) or 54 °C (unmethylation) for 30 s, and 72 °C for 20 s for 35 cycles. The amplified fragments were electrophoresed to 8% polyacrylamide gel. All the primers used for this methylation analysis were designed using MethPrimer [23]. Primers used for the first PCR and second PCR are summarized in Table 1.

For quantification, real-time PCR amplification was performed in 25 μl of reaction mixture containing 1 μl of the first PCR product (1/100 diluted with MilliQ water), 0.2 μM each primers and 12.5 μl of SYBR Green Rox Mix according to the manufacturer's protocol using iCycler iQ under the following conditions: 95 °C for 15 min for 1 cycle and 95 °C for 15 s, 57 °C (methyl) or 54 °C (unmethyl) for 15 s, 72 °C for 15 s, and fluorescent signal collection at 77 °C (methyl) or 76 °C (unmethyl) for 20 s for 40 cycles. The assay was conducted in triplicate and repeated for three times. For construction of a standard curve, serially diluted control PCR fragments were used.

Table 1
Primers used for the methylation-specific PCR

Promoter	PCR	Specification	Primer name	Primer sequence	Annealing temperature (°C)
A	1st	Bisulfite conversion specific	ERPROABSF	5′-TTAATGTTAGGGTAAGGTAATAGTTTT-3′	54
			ERPROABSR	5′-AACCACCTAAAAAAAAAACACAA-3′	
	2nd	Methylation specific	ERPROAM1F	5′-AGTTTAGGAGTTGGCGGAGGGC-3′	60
			ERPROAM1R	5′-CCGAAATTAAAAACGACGCAACG-3′	
		Unmethylation specific	ERPROAU1F	5′-GGGAGTTTAGGAGTTGGTGGAGGGT-3′	60
			ERPROAU1R	5′-ACCCAAAATTAAAAACAACACAACACA-3′	
C	1st	Bisulfite conversion specific	ERPROCBSF	5′-AGTAGATAGTAAGTTTTTTTTTATTTTTT-3′	54
			ERPROCBSR	5′-AAAAACAACCAATAAACAAAA-3′	
	2nd	Methylation specific	ERPROCM1F	5′-TTTTTTATTGTTATTTATTTAGCGT-3′	57
			ERPROCM1R	5′-AAAACACTTAACAACCCCTCCCGAC-3′	
		Unmethylation specific	ERPROCU1F	5′-TATTTTTTATTGTTATTTATTTAGTGT-3′	54
			ERPROCU1R	5′-AAACACTTAACAACCCCTCCCAAC-3′	

2.7. Bisulfite-sequencing and combined bisulfite restriction analysis (COBRA)

PCR amplification of ERα promoter C region using bisulfite-converted DNA fragments was performed as described above except for the cycle numbers to be 50. The amplified fragments were purified using NucleoSpin Extract II kit (MACHEREY-NAGEL). Direct sequencing of the fragments was conducted using ERPROCBSF as a primer, BigDye Terminators v1.1 Cycle Sequencing Kit and ABI PRISM 310 Genetic Analyzer (Applied Biosystems, Foster City, CA). For COBRA, 5 μl of purified DNA fragment was digested in a total volume of 20 μl using 5 units of *Hpy*188III restriction enzyme (New England BioLabs, Ipswich, MA) that cleave CpG sites retained because of methylation at 37 °C for 4 h. The resultant DNA fragments together with undigested ones were electrophoresed onto 8% polyacrylamide gel. After staining with ethidium bromide, the image was visualized under UV illumination. Intensity of the fluorescence of each band was quantified using ChemImager 5500 (Alpha Innotech, San Leandro, CA).

2.8. Statistical analysis

Student's *t*-test was conducted for statistical analysis. When necessary, the *t*-test was modified to all for unequal variances. *P*-values less than 0.05 were considered as significant.

3. Results

3.1. Expression levels of ERα mRNA in wild-type and LTED cells

We previously demonstrated that ERα protein and mRNA were expressed at higher levels in LTED cells than in wild-type cells using Western and Northern blot analyses [6]. As a first step, we conducted real-time PCR analysis to quantitatively evaluate ERα mRNA expression in wild-type and LTED cells: LTED cells showed 27-fold total ERα mRNA expression levels as compared with wild-type cells did ($P = 0.004$) (Fig. 1).

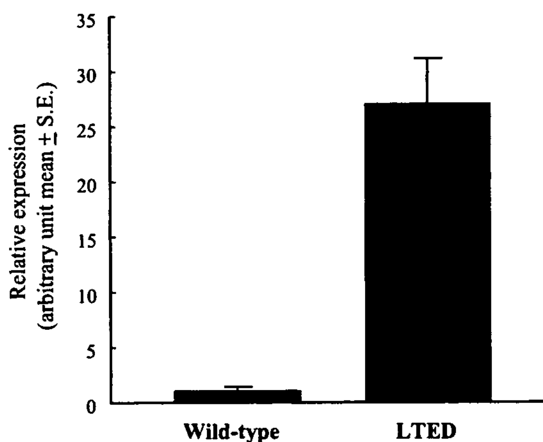

Fig. 1. Relative expression of total ERα mRNA in wild type and LTED cells. Real-time RT-PCR was conducted for quantification of total ERα and β-actin mRNA as described in Section 2. Expression levels of total ERα mRNA were normalized using β-actin mRNA.

Since an increase of ERα mRNA from promoter C was responsible for the enhanced expression of ERα protein in ERα-positive primary breast cancer and since promoter A was constitutively utilized in both normal and cancerous mammary tissue [16], we next compared ERα mRNA expression levels transcribed from these promoters A and C between wild-type and LTED cells using real-time PCR (Fig. 2). ERα mRNA from promoter A in LTED cells was 35-fold higher than that in wild-type cells ($P = 0.0007$) (Fig. 2). Furthermore, ERα mRNA expression level from promoter C in LTED was 149-fold higher than that in wild-type cells ($P = 0.01$) (Fig. 2). In wild-type cells, promoter A was dominant while promoters A and C were equally utilized in LTED cells (Fig. 2). These results indicate that reinforced utilization of promoter C in LTED cells as compared with wild-type cells may be important for the enhanced expression of ERα in LTED cells.

3.2. Transient transfection of reporter gene constructs with ERα gene promoters

The *cis*- and *trans*-acting factors are thought to generate differences in transcription activity on various promoters. We first tested the possibility that alterations of transcription factors may generate an increased level of ERα expression in LTED cells, compared with wild-type cells. We then measured the promoter activities in wild type and LTED cells using reporter gene constructs driven by ERα promoters A and C. No significant differences in promoter activities between wild-type and LTED cells were observed for these two promoters ($P = 0.3$ and 0.1 for promoters A and C, respectively, Fig. 3), suggesting that *trans*-acting factors specific to promoters A and C are not responsible for the different utilization of ERα promoters A and C between wild-type and LTED cells.

3.3. Different methylation status of ERα gene promoters in wild-type and LTED cells

We next hypothesized that alternations of higher order chromatin structure caused by DNA methylation may contribute to the expression level of ERα in these cells. Then, we compared methylation status of ERα gene promoters A and C in wild-type and LTED cells by methylation-specific PCR. Promoter A of ERα gene was unmethylated in both wild-type and LTED cells (Fig. 4). On the other hand, promoter C of ERα gene showed partial methylation in wild-type cells (Fig. 4), in good agreement with our previous report [20]. In LTED cells, the unmethylated band for promoter C was clearly observed, while the methylated one was considerably weaker (Fig. 4), in accordance with our

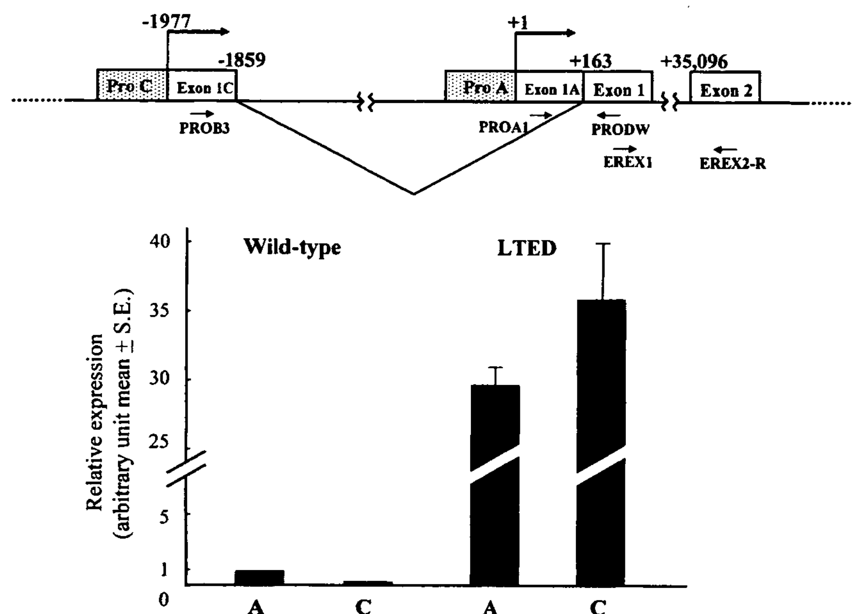

Fig. 2. Expression of ERα mRNA transcribed from promoters A and C in wild-type and LTED cells. Schematic representation of a part of ERα gene organization is shown above. The transcription start site of promoter A is defined as +1. Relative expression of ERα mRNA from promoters A and C in wild-type and LTED cells is shown. Expression levels of ERα mRNA from promoters A and C were quantified by real-time RT-PCR as described in Section 2 being normalized by β-actin mRNA.

observation that promoter C was actively utilized in LTED cells.

In order to confirm the difference of methylation status of the promoter C between wild-type and LTED cells, we next conducted direct sequencing of the PCR fragment amplified from bisulfite-converted DNA. Cytosines were predominantly observed at nucleotides −2103, −2082, and −2073 within CpG dinucleotides, while thymines are faintly detected at these sites in wild-type cells (Fig. 5). On the other hand, both thymines and cytosines were clearly observed at these sites in LTED cells (Fig. 5), confirming the difference of methylation status between wild-type and LTED cells.

3.4. *Quantitative analysis of methylation status of ERα gene promoter C in wild-type and LTED cells*

In order to quantitatively analyze the methylation of the promoter C region, we next performed two different analyses, i.e. COBRA assay and bisulfite-real-time PCR. In COBRA assay, the fragment amplified from methylated

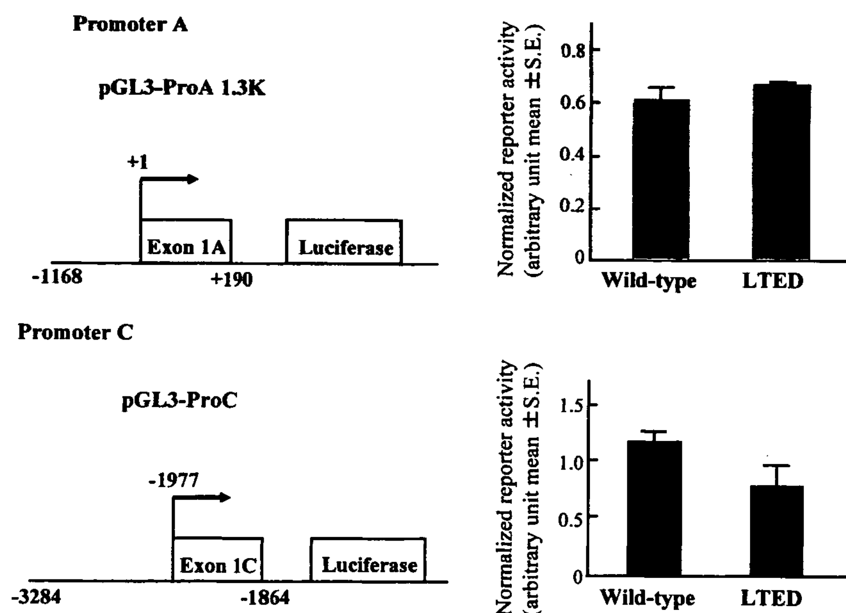

Fig. 3. Reporter activities of promoters A and C in wild-type and LTED cells. Wild-type and LTED cells were transiently transfected with a reporter gene construct pGL3-ProA 1.3K or pGL3-ProC together with control vector pRL-TK as described in Section 2. The measured luciferase activities were normalized using the control Renilla luciferase activity.

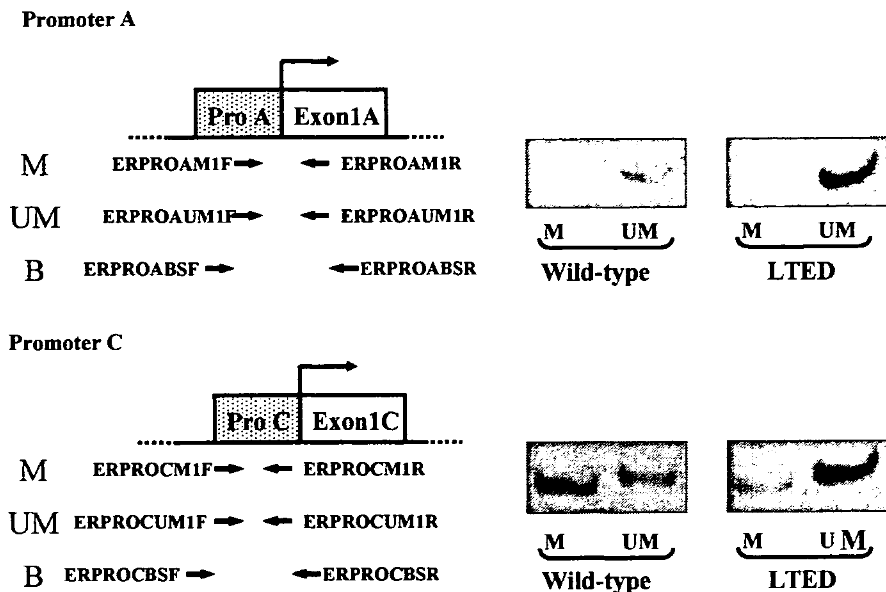

Fig. 4. Methylation-specific PCR analysis of ERα gene promoters A and C in wild-type and LTED cells. Location of primers used in methylation-specific PCR for promoters A and C is shown in the left. Photos of electrophoresis of PCR products of methylated (M) or unmethylated (UM) DNA fragments are shown in the right.

DNA can be identified as digestible bands with restriction enzyme *Hpy*188III, because of the retention of methylcytosine residue at −2073 even after bisulfite-treatment (Fig. 6). Quantification of the fragments revealed that 54% of the fragments were methylated in wild-type cells, while only 7.7% were methylated in LTED cells (Fig. 6).

This was also examined with bisulfite-real-time PCR analysis using methylation- or unmethylation-specific primers as

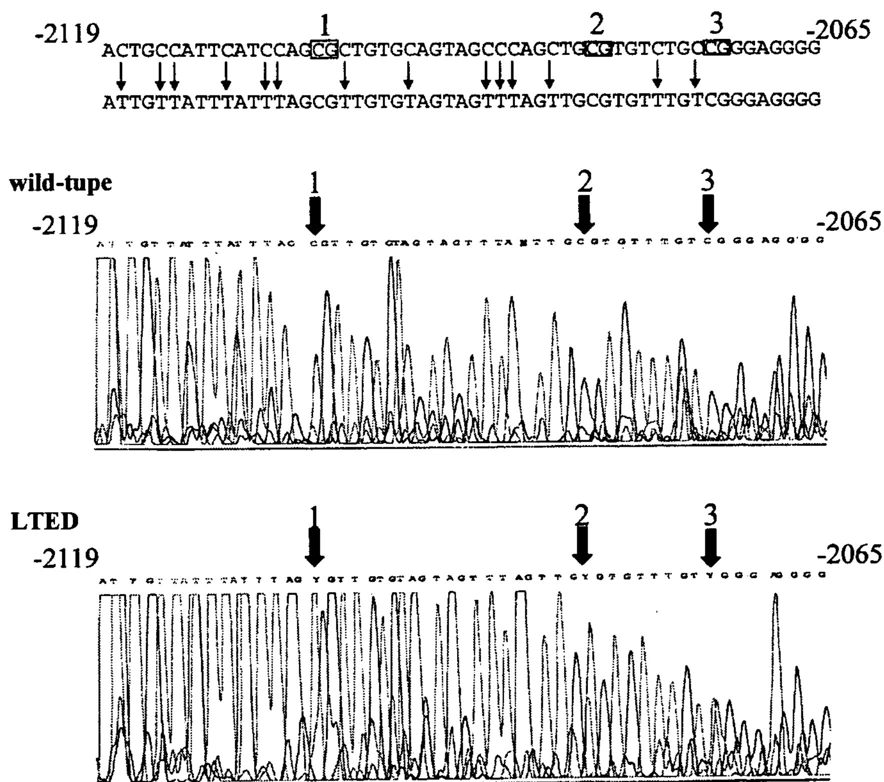

Fig. 5. Direct sequencing of PCR products of ERα gene promoter C using bisulfite-converted DNA from wild-type and LTED cells. First PCR products of bisulfite-converted DNA from wild-type or LTED cells using primers ERPROCBSF and ERPROCBSR were subjected to direct sequencing with ERPROCBSF primer as described in Section 2. Three CpG sites within the amplified region are indicated by rectangles with numbering over the rectangle. Cytosine residues that will be shown as thymine in the sequence of PCR product of bisulfite converted DNA are marked with vertical arrows in black. Thick arrows indicate the positions of three CpG sites.

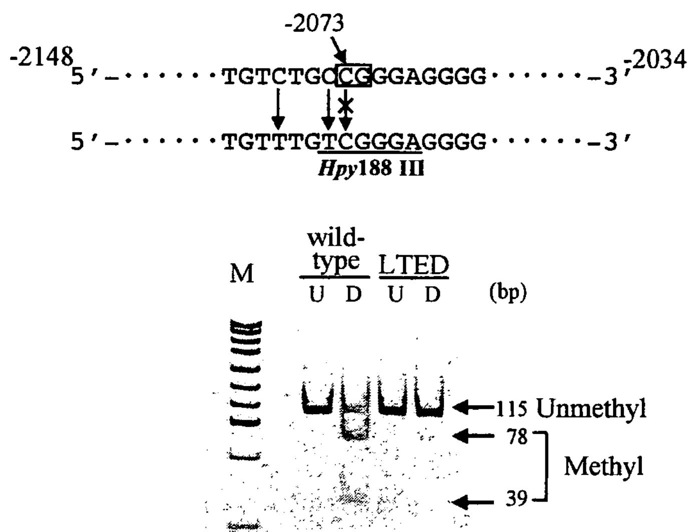

Fig. 6. COBRA assay of ERα gene promoter C in wild-type and LTED cells. First PCR products of bisulfite converted DNA from wild-type or LTED cells using primers ERPROCBSF and ERPROCBSR were digested with restriction enzyme *Hpy*188III as described in Section 2. Rectangle indicates the position of the CpG site to be tested. Underline indicates the recognition site of *Hpy*188III that will be generated by bisulfite conversion of methylated DNA, but not unmethylated one. An image of the polyacrylamide gel electrophoresis is shown below. U, untreated. D, digested with *Hpy*188III.

described above. Amount of methylated DNA in the tested sample from LTED cells was 42% of that from wild-type cells, though this was not statistically significant ($P = 0.063$) (Fig. 7). On the other hand, unmethylated DNA amount was 14.2-fold in LTED cells as compared with wild-type cells ($P < 0.001$) (Fig. 7). These results demonstrated that the promoter C region was highly unmethylated in LTED cells, but partially methylated in wild-type cells.

4. Discussion

Clinical observations suggest that human breast tumors can adapt to endocrine therapy by developing hypersensitivity to estrogen. To understand the mechanisms underlying this, we have previously examined estrogenic stimulation of cell proliferation in a model system and provided *in vitro* and *in vivo* evidence that long-term E2 ablation causes adaptive hypersensitivity. Importantly, LTED cells express ERα at a much higher level than wild cells and consequently show sub-cellular localization of ERα to the plasma membrane in addition to the nucleus. LTED cells showed higher basal estrogen responsive transcription activity as compared with wild-type cells. In addition, LTED cells activate MAP kinase signaling pathway mediated by plasma membrane-bound ERα. In both roles of ERα in the nuclei and on the plasma membranes of LTED cells, enhanced expression of

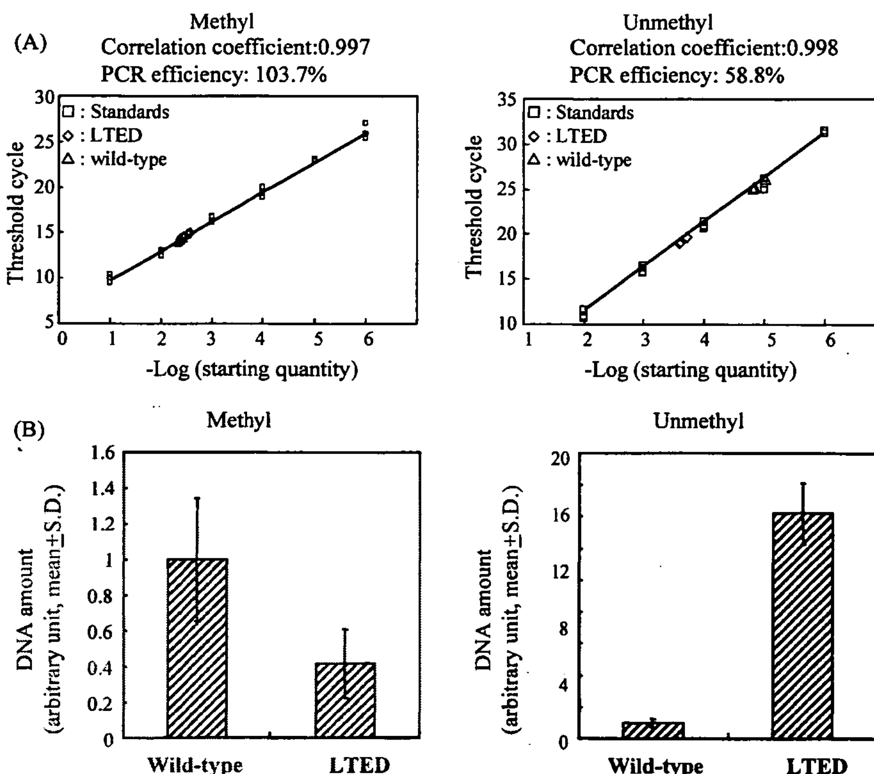

Fig. 7. Bisulfite-real-time PCR analysis of ERα gene promoter C in wild-type and LTED cells. Bisulfite-real-time PCR analysis based on SYBR-Green chemistry was conducted using methylation-specific primers ERPROCM1F and ERPROCM1R or unmethylation-specific primers ERPROCUM1F and ERPROCUM1R as described in Section 2. Representative results of bisulfite-real-time PCR are shown above. Comparison of methylated or unmethylated DNA amounts in tested samples from wild-type and LTED cells are shown below. S.D.: standard deviation.